Annals of Botany **108**: 1111–1120, 2011
doi:10.1093/aob/mcr054, available online at www.aob.oxfordjournals.org

ANNALS OF BOTANY
Founded 1887

PART OF A SPECIAL ISSUE ON FUNCTIONAL–STRUCTURAL PLANT MODELLING

Modelling fruit-temperature dynamics within apple tree crowns using virtual plants

M. Saudreau*, A. Marquier, B. Adam and H. Sinoquet

INRA, UMR 547 PIAF, F-63000 Clermont-Ferrand, France and Clermont Université, Université Blaise Pascal, UMR 547 PIAF, BP 10448, F-63000 Clermont-Ferrand, France
** For correspondence. E-mail marc.saudreau@clermont.inra.fr*

Received: 19 November 2010 Returned for revision: 4 January 2011 Accepted: 2 February 2011 Published electronically: 7 April 2011

• *Background and Aims* Fruit temperature results from a complex system involving the climate, the tree architecture, the fruit location within the tree crown and the fruit thermal properties. Despite much theoretical and experimental evidence for large differences (up to 10 °C in sunny conditions) between fruit temperature and air temperature, fruit temperature is never used in horticultural studies. A way of modelling fruit-temperature dynamics from climate data is addressed in this work.
• *Methods* The model is based upon three-dimensional virtual representation of apple trees and links three-dimensional virtual trees with a physical-based fruit-temperature dynamical model. The overall model was assessed by comparing model outputs to field measures of fruit-temperature dynamics.
• *Key Results* The model was able to simulate both the temperature dynamics at fruit scale, i.e. fruit-temperature gradients and departure from air temperature, and at the tree scale, i.e. the within-tree-crown variability in fruit temperature (average root mean square error value over fruits was 1·43 °C).
• *Conclusions* This study shows that linking virtual plants with the modelling of the physical plant environment offers a relevant framework to address the modelling of fruit-temperature dynamics within a tree canopy. The proposed model offers opportunities for modelling effects of the within-crown architecture on fruit thermal responses in horticultural studies.

Key words: Three-dimensional, 3-D, tree architecture, light interception, energy balance, phylloclimate, *Malus domestica*.

INTRODUCTION

Numerous biological processes involved in the development of fruits depend on temperature. Temperature influences fruit growth particularly the rate of cell division (Warrington *et al.*, 1999), gas exchanges (Pavel and Dejong, 1993; Lescourret *et al.*, 2000), fruit ripening (Weinberg, 1948; Marsh *et al.*, 1999; Lopez and Dejong, 2007) and fruit chemical composition (Tomes, 1963; Marsh *et al.*, 1999; Yamada *et al.*, 2004). Consequences on fruit quality such as size, colour, sugar content, acid content, nutritional quality, sunburn injury (Lakso and Kliewer, 1975; Austin *et al.*, 1999; Marsh *et al.*, 1999; Warrington *et al.*, 1999; Lobit *et al.*, 2003; Piskolczi *et al.*, 2004; Génard and Gouble, 2005; Génard *et al.*, 2007), and pest development (Kuhrt *et al.*, 2006*b*) are straightforward and well established. Thus, fruit temperature is a key parameter for fruit growth or fruit quality models.

In fruit growth models, the sensitivity to temperature is usually taken into account by degree-days accumulation as an index of physiological time (Austin *et al.*, 1999), by Q_{10} value as an estimate of respiration rate (Génard *et al.*, 2003) or more generally by allowing rates controlling biochemical reactions or cell divisions being function of temperature (Greybe *et al.*, 1998). In such models, air temperature is used instead of fruit temperature despite much theoretical and experimental evidence of large differences (up to 10 °C in sunny conditions) between fruit temperature and air temperature (Poppendiek, 1953; Thorpe, 1974; Cellier *et al.*, 1993; Saudreau *et al.*, 2009). Two main reasons could explain this fact. (1) The definition of the temperature of a fruit is not obvious since the temperature within a fruit is not uniform due to its thickness (several centimetres) and in some situations internal gradients up to 10 °C (1·5 °C cm^{-1}) were observed (Saudreau *et al.*, 2009). So the temperature of fruit cannot be estimated using one single value. (2) Even if temperature dynamics of some fruits within a canopy could be monitored via thermocouples (Saudreau *et al.*, 2009) or infrared camera (Bulanon *et al.*, 2008), it will be difficult to handle the variability in temperature dynamics of all fruits and all over the growing season. Thus, the modelling approach is appealing to overcome such difficulties and to estimate fruit temperature.

The modelling of temporal and spatial temperature variations within organs from phylloclimate was already proposed especially for fruits (Thorpe, 1974; Smart and Sinclair, 1976; Saudreau *et al.*, 2007). However such models were designed to analyse the effect of climatic factors on temperature dynamics of detached fruits. A more comprehensive analysis and modelling of the influence of the structure of trees on fruit temperature are therefore needed. Plant architecture modelling was performed for crops (maize apex, Guilioni *et al.*, 2000; maize ear, Khabba *et al.*, 1999, 2001), capitulum of sunflower (Guilioni and Lhomme, 2006) but from authors' knowledge

such efforts were not made for fruit trees. These exhibit a much higher level of complexity in term of architecture, e.g. number and spatial distribution of leaves and fruits and microclimate conditions.

Virtual plants coupled with modelling of the physical plant environment offer a relevant framework to address the modelling of fruit temperature, taking into account the fruit position within the canopy and the weather. This coupling enables several scales (i.e. from the organ to the entire plant) to be handled and quantifies the variability in the phylloclimate within a canopy (Chelle, 2005). In this paper, linking of three-dimensional (3-D) virtual tree representations with a physical-based fruit-temperature dynamical model is proposed to be able to model both the internal temperature gradients of fruit and the variability in fruit temperature within an apple tree canopy. For both scales, the model was assessed by comparing simulation results with experimental data collected in an apple orchard (Saudreau *et al.*, 2009). At the fruit scale, the assessment was done by considering fruits one by one. The variability in fruit temperature at the tree scale was assessed by considering averaged values over daytime and the ability of fruit to receive light estimated from the silhouette to total area ratio (STAR) values (Carter and Smith, 1985). The potential of this model is highlighted and discussed.

MATERIALS AND METHODS

Plant material

Three 14-year-old 'Golden Delicious' apple trees (*Malus domestica* Borkh., Rosaceae) were used. These trees were planted in an orchard of the Agroscope RAC, Centre des Fougères, Switzerland (46·14°N, 7·18°E). Each tree was trained in a different system: vertical axis (A), including a central axis bearing fruiting branches; drilling (D) made of three scaffolds; and Ycare (Y) made of two scaffolds (Fig. 1A). Within the orchard, the row orientation was north–south; inter-row distance was 4 m, with interplant distance on the row equal to 1·25 and 1 m, for A and D and Y systems, respectively. The trees were selected within the orchard so that all studied trees had neighbouring trees (Fig. 1B). In 2006, the year of the experiment, number of fruits of A, D and Y trees were 252, 278 and 202, respectively.

Microclimate measures

During 2006, a meteorological station (www.agrometeo.ch) located at 100 m from the orchard provided data of air temperature and relative humidity (model HMP45C thermo-hygrometer; Campbell Scientific, Logan, UT, USA), wind speed and direction (propeller anemometer model 5103 made by RM Young, Traverse City, MI, USA), at 2 m height. Total and diffuse PAR (R_{sky}^{PAR}) radiation from which the direct PAR radiation (R_{sun}^{PAR}) was estimated, were recorded with a BF2 sensor (Delta-T Devices Ltd, Cambridge, UK). From PAR measures, values of direct sun and diffuse sky radiations were estimated according to Varlet Grancher *et al.* (1993): 1 W of global solar radiation = 2·02 μmol s^{-1} of PAR. Sampling frequency for all these data was 10 min.

To estimate air humidity and wind flow in the orchard, both were measured in the inter-row near the digitized trees. The horizontal wind speed (hot-wire anemometers; TSI, St Paul, MN, USA) and the relative air humidity value (thermo-hygrometer HOBO© H8 Temp/RH Data Logger, ref. H08-003-02; Onset, MA, USA) were collected with a 10-min average time at 2 m above the ground.

3-D tree model

The 3-D canopy structure of the three trees was measured during summer 2006 when tree canopies were fully developed. 3-D structures were obtained using a digitizer (Fastrack, Polhemus Ltd, Cochester, VT, USA) associated with PiafDigit software (Donès *et al.*, 2006) as described in Sinoquet and Rivet (1997). The method consists of measuring the spatial co-ordinates of the proximal and distal tips of all leafy and fruiting shoots of the current year allowing shoot length and orientation to be computed. Additional 3-D digitizing measures at leaf scale (number of leaves, leaf widths and lengths, leaf angles) and shoot leaf area measures using a planimeter (LI-3100; LI-COR Biosciences, Lincoln, NE, USA) were made to derive allometric relationships, namely the relationships to infer leaves' characteristics from shoot length. Petiole length, inter-node length and leaf area along a shoot were assumed to be constant. Independent allometric relationships were computed for five types of shoot: floral growth units (30 samples), short vegetative shoots (15 samples, length <5 cm), long vegetative shoots (15 samples, length ≥ 5 cm), short bourse shoots (15 samples, length <5 cm) and long bourse shoots (15 samples, length ≥ 5 cm). These measures allowed foliage to be reconstructed according to Sonohat's method (Sonohat *et al.*, 2006). Resulting 3-D representations of 'Golden Delicious' apple trees including fruits and leaves are shown in Fig. 1A.

Light interception computation

Fruit temperature mainly depends on the amount of energy received by light (Thorpe, 1974; Smart and Sinclair, 1976; Saudreau *et al.*, 2007). The number of fruits that there are within an apple-tree canopy makes it difficult to physically measure the total amount of light that they receive. One way to estimate the amount of light received by any organ within a canopy and its dynamic, which is related to the sun position, is to process 3-D virtual plants (Sinoquet *et al.*, 1998). In this study the potential light interception by fruits was estimated by computing the silhouette to total area ratio (STAR) (Carter and Smith, 1985; Sinoquet *et al.*, 1998) of each fruit from virtual images of 3-D tree model using VegeSTAR software (Adam *et al.*, 2002). This software computes the STAR of any object within a 3-D virtual tree crown for any incident light direction. The silhouette area is the projected surface area in the incident light direction. If A is the total surface area of the fruit (for a sphere of radius r, $A = 4\pi r^2$) and A_{light} the projected surface area, the STAR is $2A_{light}/A$. The factor 2 was introduced to make sure that when half of a sphere receives light, its STAR value is 0·5. For a surface which is not shaded by any object and perpendicular to the incident light direction A_{light} is equal to $A/4$ (for a sphere $A_{light} = \pi r^2$) so

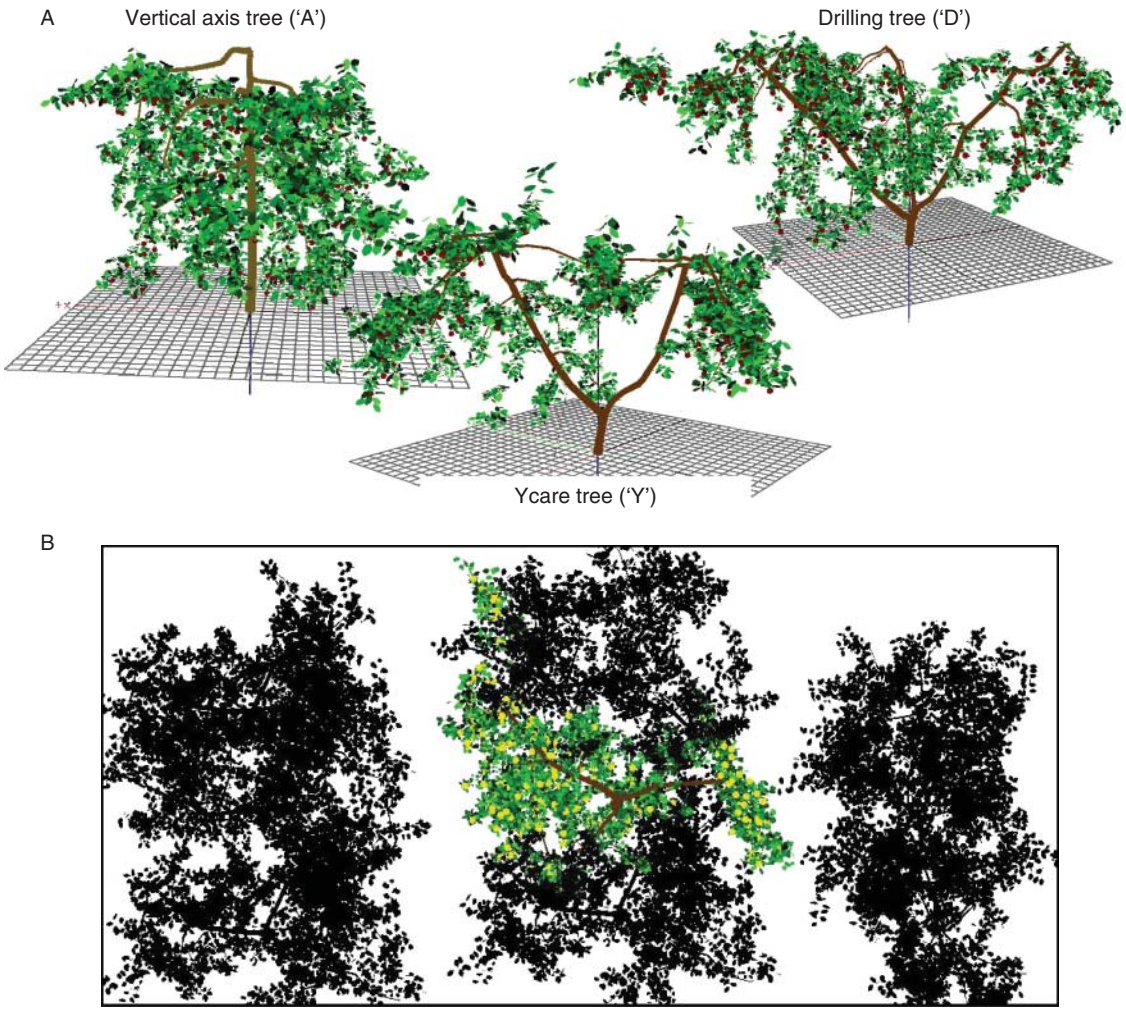

FIG. 1. Illustrations of 3-D virtual trees used to compute fruit-temperature dynamics: (A) side view of the three virtual tree architectures, and (B) top view of the virtual orchard ('Drilling' system).

the STAR value is 0·5. If half of the projected surface area is shaded by an object (e.g. by leaves, fruits or branches), A_{light} is equal to $A/8$ and the STAR value is 0·25. For a surface parallel to the incident light direction the STAR value is 0. So, for a given light direction, if the STAR value of a surface is lower than 0·5, the surface is either not perpendicular to the light direction or partially shaded by an object or both (for more details, see Sinoquet *et al.*, 1998).

Directional STAR values ($STAR_{sun}$) and a sky-integrated STAR values ($STAR_{sky}$) were calculated for each individual fruit within the tree canopy, taking into account the shading effect of other shoots and neighbouring trees (Fig. 1B). The $STAR_{sky}$ value characterized fruit light interception efficiency of diffuse radiation. For this study, the SOC (Standard OverCast) sky radiance distribution (Moon and Spencer, 1942) was used. The $STAR_{sun}$ values stood for the direct sun beam interception efficiency by a fruit and were computed for different times during daytime according to positions of the sun in the sky.

$STAR_{sun}$ and $STAR_{sky}$ values were used to compute the irradiance received by each fruit (eqn 5) and daily STAR values of each fruit by averaging STAR values over daytime with the hypothesis that direct light stands for one half of the total light ($STAR = 0{\cdot}5STAR_{sun} + 0{\cdot}5STAR_{sky}$).

Fruit-temperature measurements

Temperature measurements were carried out during spring 2006 from day of year (DOY) 204 to 205. Fruit temperature was measured with three type T copper–constantan thermocouples located on the fruit surface (bottom, T_{bottom}^{f}; top, T_{top}^{f}) and within the fruit (T_{centre}^{f}). Thermocouples were inserted under the skin to measure temperature at the fruit surface. To ensure that temperatures were measured as close as possible to fruit centres, little holes were made with a needle within each fruit. Lengths of the holes were taken equal to apple radii. Thermocouples were then inserted into holes until they reached the middle of the fruits. Thermocouples were monitored by three CR21 dataloggers (Campbell Scientific) and three 32-channel AM16/32A multiplexers (Campbell Scientific). Sampling frequency of data was 30 s and output data were averaged and stored over 20-min intervals.

To get various fruit-temperature dynamics for each tree, fruits were chosen according to their exposure to direct and

diffuse light. Thus, prior to the installation of the thermocouples, 3-D virtual trees (Fig. 1A) were used to compute the light interception – estimated from the silhouette to total area ratio denoted by STAR (Carter and Smith, 1985) – of fruits at DOY 204. Twelve fruits per tree were selected in three classes of STAR values: (0, 0·2), (0·3, 0·4) and (0·5, 0·6) (Saudreau *et al.*, 2009).

3-D fruit-temperature dynamics computation

Spatial and temporal variations of temperature in fruits were computed by solving the 3-D heat transfer equation in spherical fruits (Saudreau *et al.*, 2007):

$$\begin{cases} \frac{\partial}{\partial t}(\rho C_P.T) = \vec{\nabla}.(\vec{\vec{k}}\vec{\nabla}T) & (1a) \\ \left[-\vec{\vec{k}}\frac{\partial T}{\partial \vec{n}}\right]_r = \Phi + \lambda_E + R & (1b) \end{cases}$$

where T (K) is the temperature, ρ (kg m^{-3}) is the density, C_p (J kg^{-1} K^{-1}) is the specific heat capacity, $\vec{\nabla}$ is the spatial derivative operator, and $\vec{\vec{k}}$ (W m^{-1} K^{-1}) is the thermal conductivity of the organ. $\vec{\vec{k}}$ was assumed to be nearly isotropic, so the deviatoric part of $\vec{\vec{k}}$ was set to zero. Values of thermal and optical parameters used for simulations were measured on 'Golden Delicious' apples (Saudreau *et al.*, 2007).

Energy exchanges between the fruit and the surrounding air were modelled by specifying the normal heat flux at any point of fruit surface was equal to the loss or gain of sensible energy by convection (Φ), the loss of energy by transpirational cooling (λ_E) and the energy exchange by radiation (R) (eqn 1b). Heat fluxes were modelled as follows.

Convection:

$$\Phi = h(T_a - T_S) \quad (2)$$

where h (W m^{-2} K^{-1}) is the convective heat transfer coefficient, T_a (K) is the air temperature and T_S (K) is the unknown fruit surface temperature. For a spherical shape of radius r and under turbulent conditions, h was modelled using the Nobel's relationships (Nobel, 1975):

$$h = \left(\frac{1}{\delta} + \frac{1}{r}\right)k_{air}$$

and

$$\delta = 0{\cdot}0028\sqrt{2\frac{r}{u}} + \frac{0{\cdot}025}{u}$$

for $1{\cdot}3 \times 10^{-4}$ m^2 s$^{-1} \leq u \times r \leq 0{\cdot}5$ m^2 s^{-1}. Where k_{air} is the air thermal conductivity (= 0·0257 W m^{-1} K^{-1}) and u (m s^{-1}) is the velocity of the air.

Evaporation:

$$\lambda_E = g_w \frac{\rho_{air} C_{pair} \Delta (T_S - T_d)}{\Gamma} \quad (3)$$

where g_w (m^{-1}) is the surface conductance to water vapour diffusion, ρ_{air} is the density of the air (= 1·2 kg m^{-3}), $C_{p,air}$ is the specific heat capacity of the air (= 1010 J kg^{-1} K^{-1}), Δ is the rate of increase of saturation vapour pressure with temperature at the dew point (Monteith and Unsworth, 1990), T_d is the temperature at the dew point and Γ is the psychrometric constant (= 66·5Pa K^{-1}).

Radiation:

$$R = (1 - a_{sw})R_{sw} + (1 - a_{lw})(R_{lw} - \sigma T_s^4) \quad (4)$$

where a_{sw} and a_{lw} are the fruit surface reflectance to short-wave and long-wave radiation, respectively, $R_{lw} = \sigma T_a{}^4$ is the long-wave radiation component (TIR) and R_{sw} short-wave radiation component (PAR and NIR) of the global radiation received by a fruit, and σ is the Stefan–Boltzmann constant (= 5·67·10^{-8}J K^{-4} m^{-2} s^{-1}).

The coupling procedure

The coupling methodology was based upon the following steps (Fig. 2).

(1) For a given day, the daily sun course was split into n time steps Δt.
(2) Weather parameters (R, T_a, T_d, u) of the current day were interpolated on the time step Δt used for the sun course.
(3) The first fruit of the tree was divided into m surface elements.
(4) Using the VegeSTAR software, the direct and the diffuse light interception efficiency of each m surface element were computed taking into account the surrounding foliage distribution. $N \times m\text{STAR}_{sun}$ and $m\text{STAR}_{sky}$ values were obtained.
(5) From $n \times m\text{STAR}_{sun}$, $m\text{STAR}_{sky}$ and direct and diffuse sun radiation measures, the amount of radiation (irradiance) received by each surface element m of the fruit at time n was computed:

$$R_{sw}(n,m) = (1/0.202) \times [\sin(h)R_{sun}{}^{PAR}(n)STAR_{sun}(n,m) + R_{sky}{}^{PAR}(n)STAR_{sky}(m)] \quad (5)$$

(6) The within-fruit temperature dynamics was calculated using above heat fluxes (eqns 2–5).
(7) Go back to step 3 with another fruit.

The procedure was performed for all fruits within each tree canopy, i.e. 252, 278 and 202 fruits belonging to the A, D and Y systems, respectively.

Computation assessment and statistical analysis

Simulations were performed during 2 consecutive sunny days in 2006 (i.e. DOY 204 and 205) to assess the proposed methodology to take into account direct sun irradiance. Outputs were compared with experimental data and analysed by considering two different scales. At the fruit scale, assessment of the within-fruit gradient simulation was done by using time series of fruit-temperature dynamics. At the tree scale, the

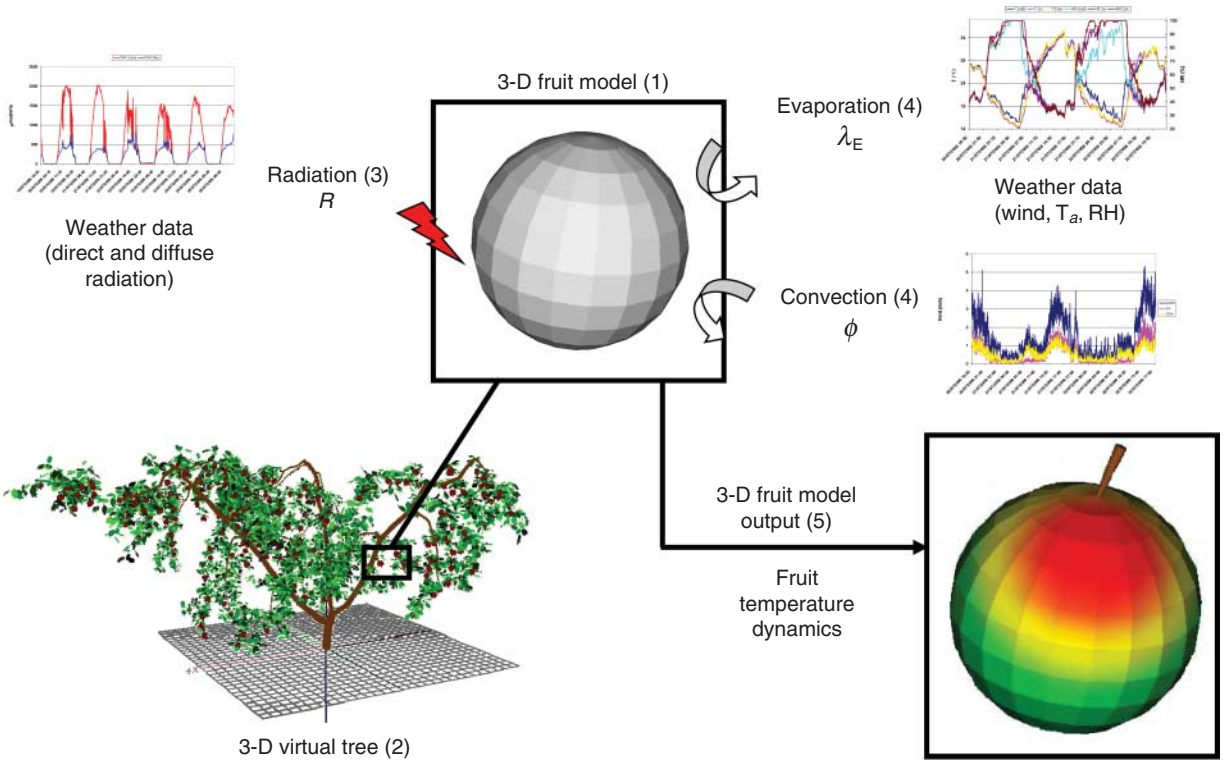

FIG. 2. Schematic representation of the coupling procedure used to compute temperature dynamics of each fruit within a tree crown. (1) Each fruit is divided into *m* surface elements. (2) Each 3-D virtual fruit is located within a 3-D virtual tree to compute direct and diffuse light interceptions of each *m* surface element taking into account the surrounding foliage distribution. (3) From light interception computation and total radiation measures, the irradiance received by each surface element *m* of each fruit is computed. (4) Other weather data (air temperature, air relative hygrometry and wind velocity) are used to compute evaporative and convective fluxes for each *m* element. (5) From radiation, convective and evaporative fluxes, the 3-D temperature dynamics within each fruit is computed.

ability of the modelling to handle the variability in fruit temperature related to the tree architecture was analysed from daily temperature [denoted by $T_{\text{bottom}}{}^{\text{f}}$ (d), $T_{\text{top}}{}^{\text{f}}$ (d) and $T_{\text{centre}}{}^{\text{f}}$ (d)] computed by averaging time series ($T_{\text{bottom}}{}^{\text{f}}$, $T_{\text{top}}{}^{\text{f}}$ and $T_{\text{centre}}{}^{\text{f}}$).

For each scale, the overall goodness-of-fit of the model was based upon the use of standard linear regression analysis (STATISTICA Software; StatSoft, Inc., Tulsa, OK, USA), including root mean square error (RMSE) defined as

$$\sqrt{\frac{\sum_{i=1}^{N}(x_i - y_i)^2}{N}}$$

where x_i is the simulated temperature and y_i the measured temperature at the time step i, and the relative RMSE, defined as relative root mean square error (RRMSE) = RMSE/$\bar{y}$ where

$$\bar{y} = \sum_{i=1}^{N} y_i / N$$

is the mean of all experimental values.

Linear regression analysis between simulation results and measures for fruit temperature for DOY 204 and 205 were computed from the multiple regression analysis toolbox of STATISTICA Software 7·0 (StatSoft Inc.).

RESULTS

Model assessment: fruit scale

The model was able to reproduce the measured temperature dynamics for the 36 monitored fruits and for the three locations within fruits. Regression analysis between observed data and simulations performed for each fruit were highly significant ($P < 0{\cdot}001$). Slopes were close to 1 : 1 with R^2 coefficients ranging from 0·848 to 0·995 (Table 1) and RMSE ranging from 0·6 °C to 2·9 °C (Table 2). RMSE values increased with increases in STAR values since RMSE were larger for the top side of fruits ($T_{\text{top}}{}^{\text{f}}$) than for the bottom side ($T_{\text{bottom}}{}^{\text{f}}$) and for larger fruit STAR values. To illustrate the ability of the integrative model to simulate the temperature dynamics of fruits within a tree crown, two instances of such dynamics are shown in Fig. 3 for two contrasting situations, i.e. sunlit and shaded fruits (STAR values above 0·4 and below 0·1, respectively). The simulation was able to reproduce the strong fluctuations in diurnal temperatures. The night-thermal dynamics was correlated with the dynamics of the air temperature whatever the fruit position within the crown, and fruits did not exhibit any temperature gradient. On the contrary, during daytime, internal gradients appeared. For a sunlit fruit (Fig. 3A, B), the difference between the temperature at the top of the fruit and at the bottom was positive during daytime and the maximum value recorded at 1400 h was 7 °C. The same trend was observed for inner gradients. The difference between the

TABLE 1. *Fruit scale: slope and* R^2 *values of the linear regression analysis between simulation results and measures for fruit temperature at DOY 204 and 205:* $T_{simulated} = aT_{measured}$

Tree	Fruit no.	Fruit STAR	Slope (R^2) of the linear regression*		
			$T_{top}{}^{f}$	$T_{centre}{}^{f}$	$T_{bottom}{}^{f}$
A	1	0·342	1·042 (0·966)	1·005 (0·982)	1·012 (0·986)
	2	0·282	1·041 (0·915)	1·017 (0·942)	1·003 (0·946)
	3	0·296	1·041 (0·925)	1·011 (0·972)	1·021 (0·980)
	4	0·276	1·006 (0·956)	0·996 (0·965)	1·001 (0·965)
	5	0·15	0·975 (0·959)	0·984 (0·980)	1·015 (0·987)
	6	0·191	1·033 (0·957)	0·985 (0·978)	0·992 (0·963)
	7	0·131	1·050 (0·926)	0·997 (0·951)	0·995 (0·967)
	8	0·103	1·005 (0·959)	0·975 (0·873)	0·977 (0·878)
	9	0·019	1·004 (0·986)	1·001 (0·965)	1·007 (0·971)
	10	0·039	0·958 (0·897)	0·981 (0·933)	0·991 (0·952)
	11	0·053	1·032 (0·957)	1·015 (0·988)	1·016 (0·988)
	12	0·058	1·017 (0·988)	1·012 (0·995)	1·016 (0·991)
D	1	0·442	1·045 (0·937)	0·992 (0·968)	1·002 (0·973)
	2	0·389	1·015 (0·985)	0·992 (0·965)	1·005 (0·978)
	3	0·338	1·021 (0·960)	0·974 (0·967)	0·990 (0·960)
	4	0·296	1·015 (0·847)	0·990 (0·949)	0·996 (0·971)
	5	0·187	1·022 (0·929)	1·002 (0·974)	1·016 (0·973)
	6	0·175	0·985 (0·926)	0·966 (0·903)	0·988 (0·952)
	7	0·198	1·007 (0·881)	0·998 (0·955)	1·011 (0·979)
	8	0·065	1·031 (0·848)	0·995 (0·950)	1·005 (0·971)
	9	0·305	0·967 (0·966)	0·977 (0·973)	1·013 (0·978)
	10	0·121	1·042 (0·962)	1·017 (0·985)	1·021 (0·978)
	11	0·072	1·032 (0·976)	1·008 (0·986)	1·013 (0·989)
	12	0·046	1·026 (0·975)	1·020 (0·988)	1·031 (0·980)
Y	1	0·312	1·013 (0·937)	0·971 (0·949)	0·981 (0·973)
	2	0·318	1·002 (0·985)	0·996 (0·98)	0·991 (0·982)
	3	0·273	0·984 (0·969)	0·980 (0·968)	0·981 (0·965)
	4	0·235	1·029 (0·969)	1·018 (0·968)	0·983 (0·974)
	5	0·125	1·009 (0·949)	0·983 (0·914)	0·993 (0·937)
	6	0·206	0·986 (0·973)	0·962 (0·948)	0·962 (0·901)
	7	0·118	0·962 (0·959)	0·987 (0·975)	1·007 (0·982)
	8	0·176	1·005 (0·950)	0·967 (0·970)	0·985 (0·974)
	9	0·042	1·009 (0·962)	1·008 (0·984)	1·022 (0·982)
	10	0·042	0·999 (0·961)	0·999 (0·979)	1·014 (0·978)
	11	0·07	1·029 (0·969)	1·017 (0·995)	1·018 (0·995)
	12	0·083	1·028 (0·978)	1·009 (0·993)	1·009 (0·994)

* All regression lines were significant (P-value $< 0{\cdot}00001$).

TABLE 2. *Fruit scale: root mean square errors (RMSE)*

Tree	Fruit no.	Fruit STAR	RMSE (°C)*			
			$T_{top}{}^{f}$	$T_{centre}{}^{f}$	$T_{bottom}{}^{f}$	Mean
A	1	0·342	2·263	1·347	0·933	1·515
	2	0·282	2·149	1·502	1·254	1·635
	3	0·296	2·397	1·360	1·011	1·589
	4	0·276	2·150	1·541	1·128	1·606
	5	0·15	2·489	1·613	0·976	1·693
	6	0·191	1·620	1·142	1·057	1·273
	7	0·131	2·229	1·252	0·973	1·485
	8	0·103	1·187	2·214	2·086	1·829
	9	0·019	0·648	0·996	0·910	0·851
	10	0·039	2·175	1·504	1·197	1·625
	11	0·053	1·466	0·788	0·781	1·012
	12	0·058	0·756	0·537	0·694	0·662
D	1	0·442	2·314	1·234	0·939	1·495
	2	0·389	1·287	1·381	0·929	1·199
	3	0·338	1·629	1·666	1·272	1·522
	4	0·296	2·857	1·552	0·961	1·790
	5	0·187	2·283	1·432	1·192	1·636
	6	0·175	2·136	2·318	1·402	1·952
	7	0·198	2·554	1·460	0·979	1·664
	8	0·065	1·647	1·389	1·225	1·420
	9	0·305	2·680	2·199	1·333	2·071
	10	0·121	1·568	0·806	0·951	1·108
	11	0·072	1·213	0·794	0·747	0·918
	12	0·046	1·084	0·795	1·091	0·990
Y	1	0·312	1·957	1·870	1·344	1·724
	2	0·318	1·246	1·044	0·984	1·091
	3	0·273	1·680	1·655	1·591	1·642
	4	0·235	1·580	1·154	1·128	1·287
	5	0·125	1·484	1·992	1·582	1·686
	6	0·206	1·423	1·920	2·105	1·816
	7	0·118	2·454	1·558	1·125	1·712
	8	0·176	1·786	2·661	2·284	2·243
	9	0·042	1·258	0·875	0·965	1·033
	10	0·042	1·424	1·113	1·070	1·202
	11	0·07	1·234	0·603	0·641	0·826
	12	0·083	1·119	0·587	0·600	0·769
Mean value			1·762	1·385	1·151	1·433

* All regression lines were significant (P-value $< 0{\cdot}00001$).

temperature measured at the top and the temperature measured at the centre was always positive during the afternoon (from 1300 to 2000 h) with a maximum value of 3 °C reached at 1430 h for both days. For shaded fruits (Fig. 3C, D), measured gradients were only +0·5 °C at noon. Finally, during daytime, fruit temperatures deviated from the temperature of the air, especially for sunlit fruits. The temperature of the upper side and the temperature of the centre were markedly above the air temperature: maximum values were +7 °C and +3 °C, respectively. Only a small deviation of the fruit temperature from the air temperature was noticed for a shaded fruit.

Model assessment: tree scale

At the tree scale, the comparison of temperature dynamics was done for each tree at the fruit centre and at the fruit surface between simulation results and measurements (Table 3). For each tree and each location within fruits, slopes of linear regression were significant (P-values $<$ 0·00001) and close to the 1 : 1 curve with R^2 coefficients ranging from 0·59 to 0·97 with lower R^2 values for the A tree. The RMSE and the RRMSE were similar for A, Y and D trees. RMSE and RRMSE varied from 1·1 °C to 2·23 °C and from 0·044 to 0·089, respectively. These statistical errors increased according to the location within the fruit, i.e. ($T_{bottom}{}^{f}$), ($T_{centre}{}^{f}$) and ($T_{top}{}^{f}$).

Linear relationships of local daily fruit temperatures, $T_{top}{}^{f}$ (d), $T_{bottom}{}^{f}$ (d), $T_{centre}{}^{f}$ (d) with daily light interception efficiency values of fruits (STAR) for both experiment and simulation were compared in Table 4. The number of fruits available on each tree from the experiment is low ($N = 12$ per tree), so all fruits were used to compute mean values without considering trees one by one. In the experiment, all linear regression equations were significant. Slope values were 5·314, 4·645 and 2·410 for $T_{top}{}^{f}$ (d), $T_{centre}{}^{f}(d)$ (d) and $T_{bottom}{}^{f}$ (d), respectively. There was no difference in intercept values. Determination coefficients R^2 were larger than 0·4 for

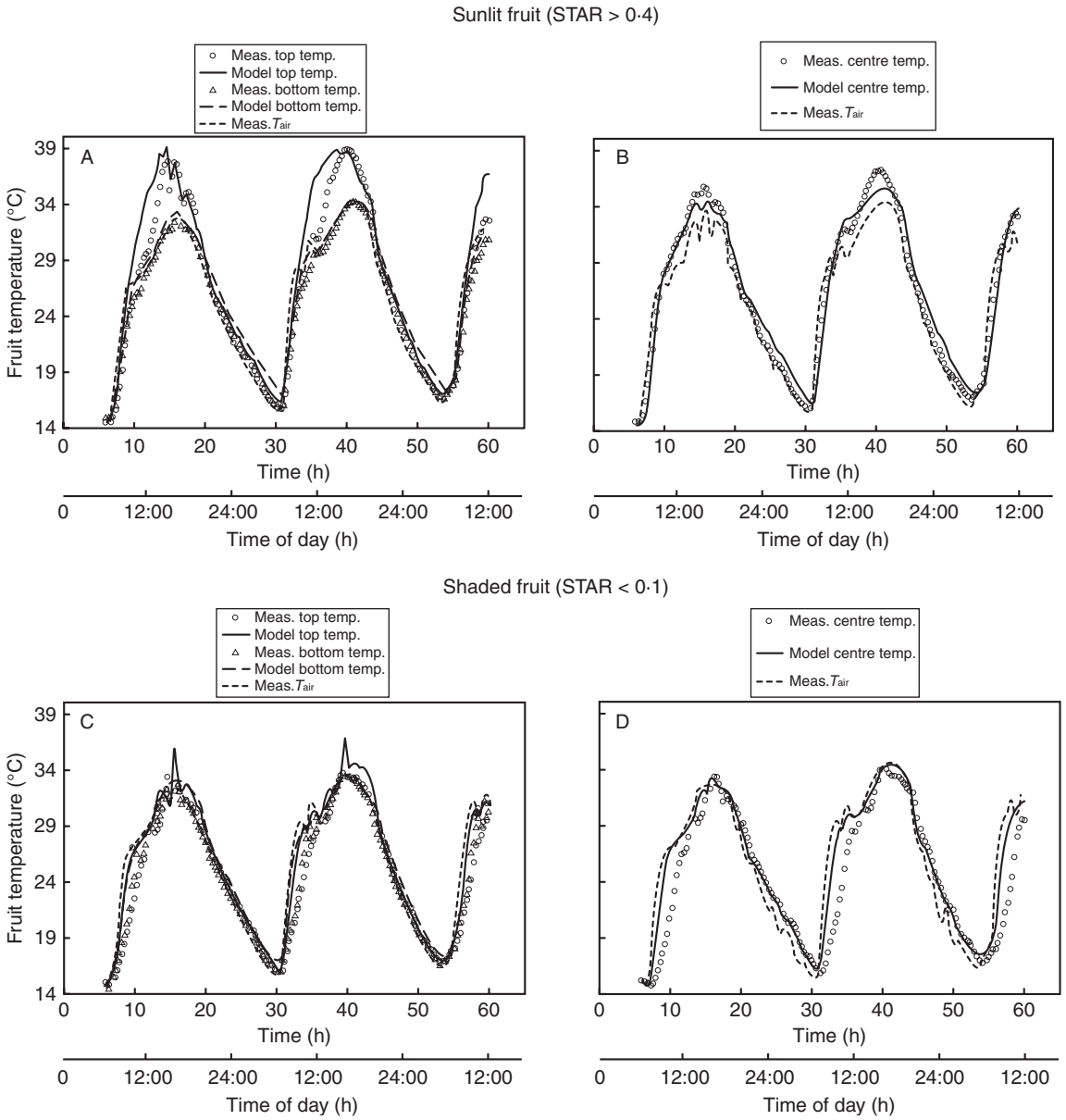

FIG. 3. Fruit-temperature dynamics during DOY 204 and 205 for a sunlit fruit (A, B) and a shaded fruit (C, D), where simulations are shown as lines, and measurements as symbols). (A) Sunlit fruit: top-side temperature, bottom-side temperature and air temperature, as indicated. (B) Sunlit fruit: centre temperature and air temperature, as indicated. (C) Shaded fruit: top-side temperature, bottom-side temperature and air temperature, as indiacted. (D) Shaded fruit: centre temperature and air temperature, as indicated.

T_{top}^{f} (d) and T_{centre}^{f} (d) and lower than 0·3 for T_{bottom}^{f} (d). Linear relationships computed from simulation results were closed to experimental results with slope values equal to 6·343, 3·810 and 1·953 for T_{top}^{f} (d), T_{centre}^{f} (d) and T_{bottom}^{f} (d), respectively. All regression lines were significant. When fruits were pooled according to STAR classes (STAR interval of 0·05), slopes were lowered but intercepts of regression equations were not changed much. Higher determination coefficients were obtained for T_{top}^{f} (d), T_{centre}^{f} (d) and T_{bottom}^{f} (d) ($R^2 > 0{\cdot}8$). Except for T_{bottom}^{f} (d) computed from experimental data since the relationship with STAR values was not significant.

DISCUSSION

Fruit scale

The integrative model was able to recover the observed fruit-temperature gradient for all fruits (Tables 1 and 2). However, at the fruit scale and whatever the fruit location within the canopy, larger errors were made for the top fruit surface temperature T_{top}^{f}. Both measure facilities and simulation assumptions were responsible for such deviations. First, as mentioned in Saudreau *et al.* (2009), measuring within-fruit temperature was tedious and it was not easy to put thermocouples perfectly at the same locations for each apple.

TABLE 3. *Tree scale: linear regression analysis between simulation results and measures for fruit temperature for DOY 204 and 205:* $T_{simulated} = aT_{measured}$

Tree	Temperature	RMSE (°C)[†]	RRMSE[‡]	Slope *a*	R^2 value	*P*-value
A	T_{top}^{f}	2·23	0·089	1·0353	0·59	<0·00001
	T_{centre}^{f}	1·37	0·0548	1·0062	0·61	<0·00001
	T_{bottom}^{f}	1·13	0·0457	1·0058	0·61	<0·00001
D	T_{top}^{f}	2·02	0·0791	1·0166	0·93	<0·00001
	T_{centre}^{f}	1·49	0·0588	0·9935	0·96	<0·00001
	T_{bottom}^{f}	1·10	0·0442	1·0072	0·97	<0·00001
Y	T_{top}^{f}	1·59	0·0630	1·0036	0·95	<0·00001
	T_{centre}^{f}	1·54	0·0609	0·9905	0·95	<0·00001
	T_{bottom}^{f}	1·38	0·0550	0·9948	0·96	<0·00001

[†] Root mean square error (RMSE).
[‡] The relative root mean square error (RRMSE = RMSE/mean of experimental values).

TABLE 4. *Linear regression analysis between fruit temperatures and fruit STAR values for simulation results and measures:* $T^{f} = aSTAR + b$ *at DOY 204 and 205*

			Slope *a*	Intercept *b*	R^2	*P*-value
Daily fruit temperature vs. STAR	Experiment	T_{top}^{f}	5·314	25·71	0·42	<0·00001
		T_{centre}^{f}	4·645	25·69	0·49	0·00002
		T_{bottom}^{f}	2·410	25·63	0·27	<0·00001
	Model	T_{top}^{f}	6·343	25·76	0·63	<0·00001
		T_{centre}^{f}	3·810	25·62	0·68	<0·00001
		T_{bottom}^{f}	1·953	25·68	0·33	<0·00001
Daily fruit temperature vs. STAR classes	Experiment	T_{top}^{f}	5·185	25·72	0·86	0·0034
		T_{centre}^{f}	4·27	25·74	0·91	0·00005
		T_{bottom}^{f}	1·87	25·74	0·43	>0·05[ns]
	Model	T_{top}^{f}	5·58	25·55	0·99	$<10^{-7}$
		T_{centre}^{f}	2·72	25·72	0·99	$<10^{-7}$
		T_{bottom}^{f}	0·83	25·81	0·99	$<10^{-7}$

[ns] not significant.

Secondly, apples were assumed to be spherical in simulations, and even if the shape of an apple fruit does not largely deviate from an ellipsoidal shape, its surface is largely curved at the vicinity of the peduncle which corresponds to the T_{top}^{f} location. At least, T_{top}^{f} dynamics is related to the dynamics of sun patches on fruit surface (Thorpe, 1974; Saudreau *et al.*, 2007). These sun patches depend on the relative position between objects surrounding fruits, e.g. leaves and the sun position in the sky. The accuracy of dynamics of sun patches is then directly linked with the foliage distribution within the canopy. In this study, only the spatial distribution of leafy and fruiting shoots were provided by the digitizing technique and positions of leaves born by these shoots were deduced from statistical relationships leading to small deviations in leaf positions in 3-D virtual trees compared with real trees (Sonohat *et al.*, 2006). Simulation errors for T_{centre}^{f} and T_{bottom}^{f} dynamics were smaller than for T_{top}^{f} because T_{centre}^{f} and T_{bottom}^{f} dynamics results from the heat diffusion process within fruits which, inherent to any diffusion process, smoothes gradients.

Tree scale

Beyond the temperature dynamics at fruit scale, this work was designed to investigate the variability in fruit temperature at the tree scale. The suggested modelling approach was successful since the variability in fruit temperature within a tree crown was recovered (Table 4). For fruit growers or horticulturists the use of daily STAR values could appear to be unclear and not useful in orchard management. Of course the use of STAR values is not straightforward because there is no experimental way to directly measure them and 3-D virtual trees are necessary for their computations (Sinoquet and Rivet, 1997). However, a STAR value is a good indicator of light received by an organ which is one of the main parameters involved in fruit quality (Volz *et al.*, 1995; Crisosto *et al.*, 1997) and, more especially, by preventing spatial co-ordinates from being used for fruit positioning (e.g. the fruit located on the north side of the tree and at 2 m high) allows different tree architectures to be compared one by one (Willaume *et al.*, 2004). The major drawback of daily STAR values is that they only stand for potential light interception and do not take into account the level of irradiance which can markedly evolve in time during 1 d (Saudreau *et al.*, 2009). As a consequence, two fruits with same daily STAR values can exhibit quite different temperatures depending on the level of irradiance received. This variability induced by the STAR definition was highlighted by the increase of R^2 coefficients of linear relationships for both model predictions and experimental values when fruits were regrouped according to STAR intervals (Table 4). In such linear relationships, the intercept is the temperature of a fruit which is always shaded

by leaves (STAR = 0). Without any energy received from the sun, its temperature should remain close to the air temperature and this is obtained in simulations (Fig. 3C, D). Slopes values of $T_{top}{}^{f}$, $T_{centre}{}^{f}$ and $T_{bottom}{}^{f}$ are also in accordance with the physics involved in fruit-temperature dynamics: (1) the more a fruit received light, the higher is its temperature, and (2) the fruit is warmed by radiation on its upper side and the heat is diffused within the fruit leading to a positive inner vertical temperature gradient: $T_{top}{}^{f} > T_{centre}{}^{f} > T_{bottom}{}^{f}$.

Conclusions

Simulations performed in this study gave accurate and relevant information in time (Fig. 3), and in space, for instance at fruit (Tables 1 and 2) and tree scales (Tables 3 and 4) on temperature dynamics of fruits within a tree canopy. Although fruit temperature is known to be a key parameter involved in fruit quality (Lakso, 1980; Yamada *et al.*, 1994), fruit sunburn injury (Glenn *et al.*, 2002) and fruit pest development (Kuhrt *et al.*, 2006*a*), no specific modelling approach has been developed so far. This suggested model could be a way to achieve this goal and could solve many horticultural questions related with fruit quality, fruit sunburn injury and fruit pest development among others. More specifically, the variability in fruit development is usually attributed to the variability in light which induces more or less photosynthetic activity in the neighbouring leaves without taking care of fruit temperature. This model takes it further by including thermal effects and by studying inter-canopy variability in terms of fruit size, quality and maturity.

Finally, this study was based upon static 3-D apple tree models to assess the modelling approach; however, this model is generic so other fruit tree species and 3-D dynamical trees commonly used in functional–structural plant modelling (Hanan and Prusinkiewicz, 2008) could be used.

LITERATURE CITED

Adam B, Donès N, Sinoquet H. 2002. VegeSTAR – software to compute light interception and canopy photosynthesis from images of 3D digitised plants. UMR PIAF INRA-UBP, Clermont-Ferrand.

Austin PT, Hall AJ, Gandar PW, Warrington IJ, Fulton TA, Halligan EA. 1999. A compartment model of the effect of early-season temperatures on potential size and growth of 'Delicious' apple fruits. *Annals of Botany* **83**: 129–143.

Bulanon DM, Burks TF, Alchanatis V. 2008. Study on temporal variation in citrus canopy using thermal imaging for citrus fruit detection. *Biosystems Engineering* **101**: 161–171.

Carter GA, Smith WK. 1985. Influence of shoot structure on light interception and photosynthesis in conifers. *Plant Physiology* **79**: 1038–1043.

Cellier P, Ruget F, Chartier M, Bonhomme R. 1993. Estimating the temperature of a maize apex during early growth stages. *Agricultural and Forest Meteorology* **63**: 35–54.

Chelle M. 2005. Phylloclimate or the climate perceived by individual plant organs: What is it? How to model it? What for? *New Phytologist* **166**: 781–790.

Crisosto CH, Johnson RS, DeJong T, Day KR. 1997. Orchard factors affecting postharvest stone fruit quality. *Hortscience* **32**: 820–823.

Donès N, Adam B, Sinoquet H. 2006. PiafDigit – software to drive a Polhemus Fastrak 3 SPACE 3D digitiser and for the acquisition of plant architecture. UMR PIAF INRA-UBP, Clermont-Ferrand.

Génard M, Gouble B. 2005. ETHY: a theory of fruit climacteric ethylene emission. *Plant Physiology* **139**: 531–545.

Génard M, Lescourret F, Gomez L, Habib R. 2003. Changes in fruit sugar concentrations in response to assimilate supply, metabolism and dilution: a modeling approach applied to peach fruit (*Prunus persica*). *Tree Physiology* **23**: 373–385.

Génard M, Bertin N, Borel C, *et al*. 2007. Towards a virtual fruit focusing on quality: modelling features and potential uses. *Journal of Experimental Botany* **58**: 917–928.

Glenn DM, Prado E, Amnon E, McFerson J, Puterka GJ. 2002. A reflective, processed-kaolin particle film affects fruit temperature, radiation reflection, and solar injury in apple. *Journal of the American Society for Horticultural Science* **127**: 188–193.

Greybe E, Bergh O, Ferreira D. 1998. Fruit growth and cell multiplication of Royal Gala apples as a function of temperature. *Applied Plant Science* **12**: 10–14.

Guilioni L, Lhomme JP. 2006. Modelling the daily course of capitulum temperature in a sunflower canopy. *Agricultural and Forest Meteorology* **138**: 258–272.

Guilioni L, Cellier P, Ruget F, Nicoullaud B, Bonhomme R. 2000. A model to estimate the temperature of a maize apex from meteorological data. *Agricultural and Forest Meteorology* **100**: 213–230.

Hanan P, Prusinkiewicz P. 2008. Special Issue: Functional–Structural Plant Modelling. *Functional Plant Biology* **35**: 1–1090.

Khabba S, Ledent JF, Lahrouni A. 1999. Development and validation of model of heat diffusion in maize ear. *Agricultural and Forest Meteorology* **97**: 113–127.

Khabba S, Ledent JF, Lahrouni A. 2001. Maize ear temperature. *European Journal of Agronomy* **14**: 197–208.

Kuhrt U, Samietz J, Dorn S. 2006*a*. Effect of plant architecture and hail nets on temperature of codling moth habitats in apple orchards. *Entomologia Experimentalis et Applicata* **118**: 245–259.

Kuhrt U, Samietz J, Dorn S. 2006*b*. Thermal response in adult codling moth. *Physiological Entomology* **31**: 80–88.

Lakso AN. 1980. Correlations of fisheye photography to canopy structure, light climate, and biological responses to light in apple trees. *Journal of the American Society for Horticultural Sciences* **105**: 43–46.

Lakso AN, Kliewer WM. 1975. The influence of temperature on malic acid metabolism in grape berries: I. Enzyme responses. *Plant Physiology* **56**: 370–372.

Lescourret F, Inizan O, Génard M. 2000. Analyse de l'étalement temporel de la floraison et influence de la variabilité intra-arbre de la chute et de la croissance précoce des pêches. *Canadian Journal of Plant Science* **80**: 129–136.

Lobit P, Génard M, Wu BH, Soing P, Habib R. 2003. Modelling citrate metabolism in fruits: responses to growth and temperature. *Journal of Experimental Botany* **54**: 2489–2501.

Lopez G, Dejong TM. 2007. Spring temperatures have a major effect on early stages of peach fruit growth. *Journal of Horticultural Science & Biotechnology* **82**: 507–512.

Marsh KB, Richardson AC, Macrae EA. 1999. Early- and mid-season temperature effects on the growth and composition of satsuma mandarins. *Journal of Horticultural Science and Biotechnology* **74**: 443–451.

Monteith JL, Unsworth MH. 1990. *Principles of environmental physics*. London: Edward Arnold.

Moon P, Spencer DE. 1942. Illumination from a non-uniform sky. *Transactions of the Illumination Engineering Society* **37**: 707–726.

Nobel PS. 1975. Effective thickness and resistance of the air boundary layer adjacent to spherical plant parts. *Journal of Experimental Botany* **26**: 120–130.

Pavel EW, Dejong TM. 1993. Seasonal CO_2 exchange patterns of developing peach (*Prunus persica*) fruits in response to temperature, light and CO_2 concentration. *Physiologia Plantarum* **88**: 322–330.

Piskolczi M, Varga C, Racsko J. 2004. A review of the meteorological causes of sunburn injury on the surface of apple fruit (*Malus domestica* Borkh). *Journal of Fruit and Ornamental Plant Research* **12**: 245–252.

Poppendiek H. 1953. Transient and steady-state heat transfer in irradiated citrus fruit. *Transactions of the ASME* **75**: 421–425.

Saudreau M, Sinoquet H, Santin O, *et al*. 2007. A 3D model for simulating the spatial and temporal distribution of temperature within ellipsoidal fruit. *Agricultural and Forest Meteorology* **147**: 1–15.

Saudreau M, Marquier A, Adam B, Monney P, Sinoquet H. 2009. Experimental study of fruit temperature dynamics within apple tree crowns. *Agricultural and Forest Meteorology* **149**: 362–372.

Sinoquet H, Rivet P. 1997. Measurement and visualization of the architecture of an adult tree based on a three-dimensional digitising device. *Trees – Structure and Function* **11**: 265–270.

Sinoquet H, Thanisawanyangkura S, Mabrouk H, Kasemsap P. 1998. Characterization of the light environment in canopies using 3D digitising and image processing. *Annals of Botany* **82**: 203–212.

Smart RE, Sinclair TR. 1976. Solar heating of grape berries and other spherical fruits. *Agricultural Meteorology* **17**: 241–259.

Sonohat G, Sinoquet H, Kulandaivelu V, Combes D, Lescourret F. 2006. Three-dimensional reconstruction of partially 3D-digitized peach tree canopies. *Tree Physiology* **26**: 337–351.

Thorpe MR. 1974. Radiant heating of apples. *Journal of Applied Ecology* **11**: 755–760.

Tomes ML. 1963. Temperature inhibition of carotene synthesis in tomato. *Botanical Gazette* **11**: 180–185.

Varlet Grancher C, **Bonhomme R**, **Sinoquet H**, eds**. 1993.** *Crop structure and light microclimate: characterization and applications*. Paris: INRA Editions.

Volz RK, Palmer JW, Gibbs HM. 1995. Within-tree variability in fruit quality and maturity for 'Royal Gala' apple. *Acta Horticulturae* **379**: 67–74.

Warrington IJ, Fulton TA, Halligan EA, Silva HND. 1999. Apple fruit growth and maturity are affected by early season temperatures. *Journal of the American Society for Horticultural Science* **124**: 468–477.

Weinberg JH. 1948. Influence of temperature following bloom on fruit development period of 'Elberta' peach. *Proceedings of the American Society for Horticultural Science* **51**: 175–178.

Willaume M, Lauri PE, Sinoquet H. 2004. Light interception in apple trees influenced by canopy architecture manipulation. *Trees – Structure and Function* **18**: 705–713.

Yamada H, Ohmura H, Arai C, Terui M. 1994. Effect of preharvest fruit temperature on ripening, sugars, and watercore occurrence in apples. *Journal of the American Society for Horticultural Science* **119**: 1208–1214.

Yamada H, Takechi K, Hoshi A, Amano S. 2004. Comparison of water relations in watercored and non-watercored apples induced by fruit temperature treatment. *Scientia Horticulturae* **99**: 309–318.